Phys. Status Solidi RRL **8**, No. 6, 566–570 (2014) / **DOI** 10.1002/pssr.201409048

Part of Focus Issue on
Functional Oxides
Eds.: T. Frauenheim, J. M. Knaup, P. Broqvist, S. Ramanathan

pss +++rapid research letters+++
www.pss-rapid.com

Theoretical study of charge separation at the rutile–anatase interface

Jolla Kullgren, Huynh Anh Huy, Bálint Aradi, Thomas Frauenheim, and Peter Deák*

Bremen Center for Computational Materials Science, Universität Bremen, P.O. Box 330440, 28334 Bremen, Germany

Received 27 January 2014, revised 4 March 2014, accepted 4 March 2014
Published online 11 March 2014

Keywords TiO_2, band offsets, carrier trapping, vacancies, density functional theory

* Corresponding author: e-mail deak@bccms.uni-bremen.de, Phone: +49-421-218-62353, Fax: +49-421-218-62770

Mixed phase TiO_2 powders are very effective in photocatalysis. It is assumed that this efficiency is connected to the separation of photogenerated mobile electrons and holes between rutile and anatase, controlled by the offsets between their valence and conduction bands. The actual alignment is, however, debated. Our high level electronic structure calculations suggest that, at typical rutile/anatase interfaces, the band edges of rutile lie higher in energy than those of anatase. This conclusion is reached by taking into account the generic alignment of the bulk band structures and the specific structure of the interface. The latter has been obtained by simulated annealing, using approximate quantum mechanical molecular dynamics on models of the rutile(100)/anatase(100) and of the rutile(110)/anatase(101) interface. Our results are corroborated by photoelectron spectroscopy of actual rutile/anatase interfaces in the literature. The predicted band offsets would lead to accumulation of mobile electrons in anatase and mobile holes in rutile, with the process being also supported by electron self-trapping in rutile and hole self-trapping in anatase. We show, however, that interface defects, like the oxygen vacancy, may provide a recombination channel. Such effects may explain the variation in the suggested direction of charge transfer in many experiments.

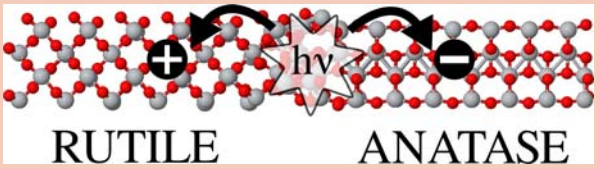

The rutile(100)/anatase(100) interface. Titanium atoms are drawn with gray and oxygen with red circles. The black arrows show the preferred direction in the charge transfer of photogenerated electrons and holes.

1 Introduction Ever since Fujishima and Honda [1] discovered the photocatalytic properties of titania (TiO_2), much research has been focused on its potential use in environmental- and energy-related technologies. Consequently TiO_2 is found in a large number of applications such as heterogeneous catalysis, photocatalysis, fuel cells, electronic gas sensors, optoelectronics, or photovoltaics. The two most important forms of TiO_2 are rutile and anatase. While, anatase is generally considered to be the more photoactive of the two, mixtures (mixed-phase TiO_2 from here on), exhibit even higher photoactivity than the pristine forms. The effect is believed to be connected to the separation of photoexcited charge carriers, with electrons residing in one phase and holes in the other. This separation of charge relies on a good contact between rutile and anatase particles in mixed-phase TiO_2 [2, 3].

It is generally believed, that the enhanced charge separation is largely due to a staggered band offset between the two modifications, which have different band gaps. The alignment of the bands between the phases is, however, still a matter of debate. Different experiments have led to varying assumptions on the band offsets. Correspondingly, some of these studies [4–8] suggest that the key in the synergism is electron transfer from rutile to anatase, others [9–13] refer to the opposite direction. We would like to point out that most of these experiments provide only indirect evidence, and a number of assumptions are necessary to deduce the band offsets. Direct information about those

can only be obtained from photoelectron spectroscopy of actual interfaces, but due to the difficulty of creating well-defined model anatase/rutile systems, that are amenable to experimental techniques, such studies are scarce [14]. Therefore, we will not scrutinize the experimental literature here. Instead, based on theoretical investigations, we describe three factors, influencing the charge transfer between the two phases:

- the alignment of the conduction and valence bands of rutile and anatase across specific interfaces, i.e., the *band offsets*,
- the effect of *self-trapping* of charge carriers, which is different in rutile and anatase, and
- the role of *oxygen vacancies near the interface*.

We will show, that the first two favor the accumulation of mobile electrons in anatase and mobile holes in rutile, while the third provides a channel for counteracting the separation.

The band offsets across an interface are determined on the one hand by the generic alignment of the bulk band structures and, on the other, by the actual structure (dipole layer, charged defects, etc.) of the interface. The former has been reported in three recent theoretical studies [15–17], based on accurate bulk band structure calculations with a hybrid functional. The alignment was done in several different ways, using charge neutrality levels (branching point energies), the Mott–Littleton approach, ionization potentials, or electrostatic potentials in the two phases. These three studies consistently give a staggered band alignment with the valence/conduction band edges of anatase being 0.55/0.35 eV [15], 0.47/0.30 eV [16] or 0.63/0.39 eV [17] below the respective band edges of rutile, see Fig. 1 and Table 1. The studies of Scanlon et al. and Pfeifer et al. also provided experimental evidence from X-ray photoelectron spectroscopy (XPS) measurements in support of the calculations, yielding valence/conduction band offsets of 0.39/0.22 eV [16] and 0.7/0.5 eV [17], respectively, with anatase at lower energies. Such a staggered band alignment would mean that photogenerated electrons in mixed-phase TiO_2 could readily transfer from rutile to anatase.

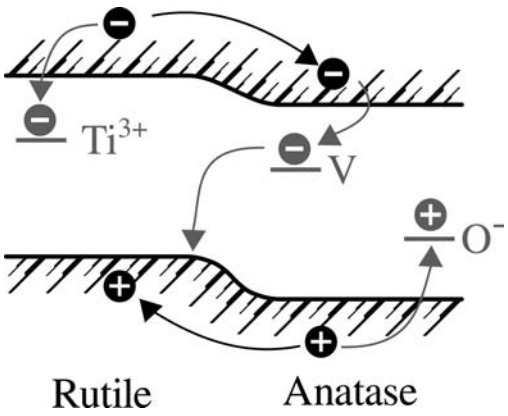

Figure 1 Schematic illustration of the staggered band alignment of rutile and anatase. The general direction of charge transfer in absence of self-trapping and near interface defects is shown in black. Self-trapping levels and back-transfer from near interface oxygen vacancies is shown in gray.

Table 1 Alignment of the electronic structures of rutile and anatase. Jump in the average electrostatic potential at the interface (ΔV) and the valence/conduction band offset (VBO/CBO), i.e. the energy position of the valence band edge of rutile over that of anatase is given for two specific interfaces, R(100)/A(100) and R(110)/A(101), in comparison with the generic offset of the bulk valence band edges.

interface	ΔV (eV)	VBO (eV)	CBO (eV)
R(100)/A(100)	1.11	0.86	0.65
R(110)/A(101)	1.08	0.90	0.69
R/A bulk (Ref. [15])	–	0.55	0.35
R/A bulk (Ref. [16])	–	0.47	0.30
R/A bulk (Ref. [17])	–	0.63	0.39

This picture might, however, change if the structure of the actual interface is taken into account. Therefore, we present theoretical predictions for the band offsets across two specific structurally optimized interfaces between anatase and rutile.

2 Methods Molecular dynamic calculations were carried out using the self consistent charge density functional tight binding scheme (SCC-DFTB [18]) using the DFTB + code [19]. SCC-DFTB is an approximate DFT approach derived from a second-order expansion of the DFT energy with respect to charge density fluctuations. In the current investigation we have used the Ti-O parameters, *tiorg* [20], developed by Dolgonos et al. in Ref. [21].

Final relaxation of the interface models and determination of the electrostatic potential were carried out by *ab initio* DFT calculations using the Perdew–Burke–Ernzerhof (PBE) functional [22][1]. Band structures of the bulk phases have been obtained with the hybrid functional of Heyd, Scuseria and Ernzerhof (HSE06) [23]. For both types of calculations the Vienna Ab-initio Simulation Package (VASP) [24, 25] was used. A cutoff of 420 eV was imposed for the plane-wave basis-set describing the valence electrons (10 for titanium and 6 for oxygen), while the core electrons were treated with the Projector Augmented Wave method (PAW) developed by Blöchl [26]. In the slab calculations only the Γ-point was used in the sampling of the Brillouin zone, while in the bulk Monkhorst–Pack grids of 8 × 8 × 12 and 8 × 8 × 4 were applied for rutile and anatase, respectively. In all slab calculations a vacuum layer of at least 12 Å were applied in order to reduce inter-

[1] Unfortunately, a HSE calculation for the interface model is not yet possible. Since PBE commits the same error in the two modifications of TiO_2, the jump in the electrostatic potential is expected to be reliably predicted by PBE, with an error well within the accuracy of such a model calculation.

actions between mirror images. For determining the average potential across the interface, the vacuum layer has been doubled. Dipole corrections were applied for all slabs.

The surface unit cell of the slabs for modeling the interfaces was p(4 × 2)/p(3 × 1) and c(6 × 4)/p(4 × 3) for R(100)/A(100) and R(110)/A(101), respectively. In the annealing, the rutile/anatase parts contained 6/8 TiO_2-layers in the former and 6/5 layers in the latter case. The outermost two molecular layers were held fixed. After annealing 6/8 and 2/2 layers have been added to the rutile/anatase end, and relaxed with *ab initio* DFT without any constraint. The final models corresponds to $Ti_{192}O_{384}$ and $Ti_{360}O_{720}$, respectively.

3 Results and discussion We have investigated the R(100)/A(100) interface, arising between the (100) surface of rutile (R) and the (100) surface of anatase (A), as well as the R(110)/A(101) interface. The first involves reactive facets of high surface energy, leading to the strongest adhesion [27], while the second involves the thermodynamically most stable surface facets. In a 2D-periodic model of the interface, the surface supercells were selected in order to keep the strain, due to lattice mismatch, as low as possible, while keeping the system size computationally tractable. The lattice mismatch was about 4% in both cases[2]. The work of Deskins et al. [27] has shown that a substantial reduction of the mismatch would require supercells larger than the usual grain size in mixed phase TiO_2.

As mentioned in the Introduction, it has been recognized that efficient charge separation in mixed-phaseTiO_2 necessitates a good contact between rutile and anatase particles [7, 10, 28]. To achieve such bonding, each interface was subjected to simulated annealing, using semi-empirical quantum molecular dynamics[3]. For more details see Section 2. The temperature program of the annealing included a linear ramp from 0 K to 2250 K over 10 ps, followed by equilibration at the constant temperature of 2250 for 40 ps, and an exponential cooling curve down to 0 K. Throughout the annealing process the outer ends of the slab were kept fixed, allowing the use of this high temperature to accelerate the contact formation. While the annealing time is still much too short for diffusion to take place even at this temperature, coordination analysis of the Ti atoms as a function of annealing time has shown that the system is equilibrated by the end of the process. The interface after annealing is dominated by tetrahedrally coordinated Ti atoms, in agreement with experiments showing their evolution in mixed phase TiO_2 samples [29]. After annealing, a number of additional layers of rutile and anatase were added to the corresponding outer ends. These extended slabs were then relaxed without constraint using *abinito* density functional theory (DFT) at the semi-local level of approximation (see Section 2 for details). The resulting structures are shown in Figs. 2 and 3, together with the electrostatic potential averaged over planes parallel to the interface. By using Gaussian smearing (blue line), the layer-to-layer average of the potential can be readily obtained.

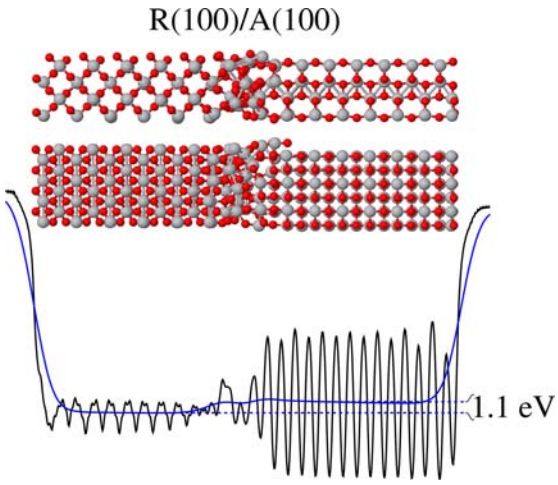

Figure 2 Fully relaxed R(100)/A(100) interface. The structure is shown from two sides with titanium atoms drawn with gray and oxygen atoms with red circles. The average potential along the interface, with (blue dashed line) and without Gaussian smearing (black solid line), is shown in the graph below the structure. The calculated potential jump across the interface is given in eV.

This potential curve shows a jump of 1.11 eV at the R(100)/A(100) and of 1.08 eV at the R(110)/A(101) inter-

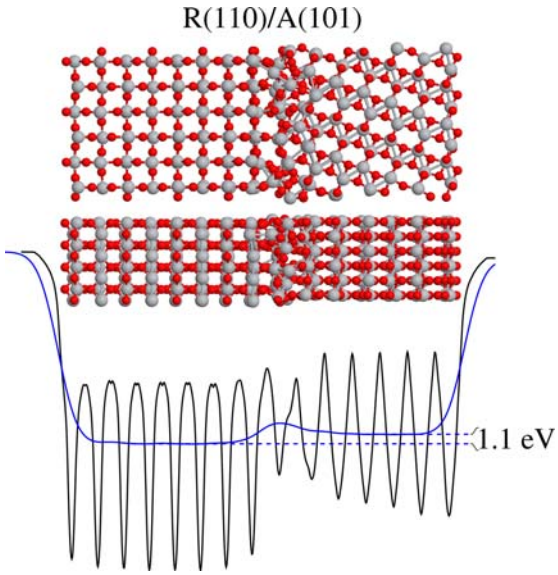

Figure 3 Fully relaxed the R(110)/A(101) interface in a similar display as in Fig. 2.

[2] Synthesis under non-equilibrium conditions might produce even higher strain, but that should lead to a very disordered surface, with less resulting dipole moment, then the chosen ones, and to worse electrical contact, which is, however, crucial to the synergic effect, see Refs. [2, 3].

[3] In order two obtain plausible models of the rutile/anatase interface, we "weld" rutile and anatase slabs by simulated annealing.

face, with the average being lower in rutile. As a validation of our results, we calculated the potential differences between the "bulk" parts of the slab and the vacuum, and compared them with the corresponding values from separate rutile and anatase slabs. We find only minor differences, indicating that the slab used for modeling the interface is large enough to separate the effect of the interface from that of the outer surfaces.

To obtain the valence band offset across the interfaces, we need to know the energy difference between the valence band edge and the average electrostatic potential in both phases [30]. We have obtained this from 3D-periodic bulk calculations using an accurate hybrid functional, as described in Section 2. The valence band edge lies 12.08 eV above the average electrostatic potential in rutile and by 10.11 eV in anatase. Taking into account the potential jump at the interface, this leads to the valence band offsets shown in Table 1. Using the calculated values for the bulk band gaps (which agree well with experiment) [15] the conduction band offset is 0.65 eV at the R(100)/A(100) and 0.69 eV at the R(110)/A(101) interface. Qualitatively, the band offsets at both interfaces are in the same direction as the generic band offset obtained by aligning the band structures without consideration of the interface (see Fig. 1), only slightly larger. Therefore, we are confident that the most common interfaces in mixed phase TiO_2 will lead to the transfer of photoexcited electrons and hole to anatase and rutile, respectively.

The accumulation of one type of mobile carriers in each of the phases is, however, also influenced by carrier trapping, with different mechanisms in the two phases. Theoretical studies of Deák et al. [31, 32], in comparison with experimental information on dopants and oxygen vacancies, have clearly demonstrated self-trapping of mobile electrons in rutile (converting Ti^{4+} into Ti^{3+}) and self-trapping of mobile holes in anatase (converting O^{2-} into O^{-}), but not vice versa. The combined consequence of the staggered band alignment and the differing self-trapping mechanisms is depicted in Fig. 1. Electrons excited into the conduction band of rutile near the interface are likely to slide down into the conduction band of anatase, while electrons excited far from the interface are likely to be trapped in the bulk of rutile. Similar arguments hold for holes created in anatase. Therefore, both the band alignment and the self-trapping of carriers contribute to the accumulation of mobile electrons in anatase and mobile holes in rutile, giving rise to effective charge separation between the phases.

Finally, we will consider the effect of the most common defect in TiO_2, i.e., the oxygen vacancy. Theoretical investigations [32] have shown that oxygen vacancies are predominantly found in a positive charge state at room temperature. In rutile (unless very strongly reduced) oxygen vacancies autoionize in favor of Ti^{4+}/Ti^{3+} traps in their neighborhood, i.e., they do not give rise to mobile electrons. In contrast, there is no electron self-trapping in anatase, and the donor level of the oxygen vacancy is very shallow so, in bulk anatase, they easily release one electron to the conduction band. If, however, the vacancy is sufficiently close to the interface, its donor electrons can recombine with free holes in the valence band of rutile. The now empty vacancy level can then be replenished by electrons arriving from rutile into the conduction band of anatase. This way, an oxygen vacancy near the interface in anatase acts as a recombination center, channeling electrons back to rutile, and effectively quenching the charge separation. This mechanism may explain the experimental findings of Komaguchi et al. [12] showing an increased transfer of electrons from anatase to rutile in reduced samples of mixed phase TiO_2.

Our results on the charge separation in mixed-phase TiO_2 are summarized in Fig. 1. Photogenerated electron hole pairs will be separated in mixed phase TiO_2 by the alignment of the band structures of rutile and anatase at the most important interfaces. Mobile electrons will be accumulating in anatase and mobile holes in rutile. This result is consistent with experimental observation of larger charge transfer in mixed-phase TiO_2 with smaller average particle sizes [7]. The separation of mobile carriers is reinforced by the inherent self-trapping mechanisms for electrons in rutile and holes in anatase. In contrast, the presence of oxygen vacancies near the interface counteracts the separation, and provide a channel for electron transfer from anatase to rutile. This last effect shows that the net charge transfer can very much depend on the microscopic structure of the interface, i.e. on the preparation of a specific mixture. That might explain the varying conclusions of different experiments. However, our present work, together with those in Refs. [15–17], firmly establishes the band alignment of Fig. 1 between rutile and anatase particles in direct (electronic) contact with each other. Work on the theoretical interpretation of indirect experiments (based on measurements on separate rutile and anatase samples) is in progress.

Acknowledgements This work has been supported by the Grant HHB15 at the Julich Supercomputer Centre (JSC). J.K. acknowledges the support of the Hanse-Wissenschaftskolleg (HWK) and useful discussions with Matthew Wolf.

References

[1] A. Fujishima and K. Honda, Nature **238**(5358), 37–38 (1972).
[2] T. Ohno, K. Sarukawa, K. Tokieda, and M. Matsumura, J. Catalysis **203**(1), 82–86 (2001).
[3] G. Li, L. Chen, M. E. Graham, and K. A. Gray, J. Mol. Catalysis A **275**(1–2), 30–35 (2007).
[4] D. C. Hurum, A. G. Agrios, K. A. Gray, T. Rajh, and M. C. Thurnauer, J. Phys. Chem. B **107**(19), 4545–4549 (2003).
[5] T. Ohno, K. Tokieda, S. Higashida, and M. Matsumura, Appl. Catalysis A **244**(2), 383–391 (2003).
[6] D. C. Hurum, K. A. Gray, T. Rajh, and M. C. Thurnauer, J. Phys. Chem. B **109**(2), 977–980 (2005).

[7] D. Hurum, A. Agrios, S. Crist, K. Gray, T. Rajh, and M. Thurnauer, J. Electron Spectrosc. Relat. Phenom. **150**(2–3), 155–163 (2006).
[8] G. Li, C. P. Richter, R. L. Milot, L. Cai, C. A. Schmuttenmaer, R. H. Crabtree, G. W. Brudvig, and V. S. Batista, Dalton Trans. **45**, 10078–10085 (2009).
[9] T. Kawahara, Y. Konishi, H. Tada, N. Tohge, J. Nishii, and S. Ito, Angew. Chem. Int. Ed. **41**(15), 2811–2813 (2002).
[10] T. Miyagi, M. Kamei, T. Mitsuhashi, T. Ishigaki, and A. Yamazaki, Chem. Phys. Lett. **390**(4–6), 399–402 (2004).
[11] H. Nakajima, T. Mori, Q. Shen, and T. Toyoda, Chem. Phys. Lett. **409**(1–3), 81–84 (2005).
[12] K. Komaguchi, H. Nakano, A. Araki, and Y. Harima, Chem. Phys. Lett. **428**(4–6), 338–342 (2006).
[13] X. Zhang, Y. Lin, D. He, J. Zhang, Z. Fan, and T. Xie, Chem. Phys. Lett. **504**(1–3), 71–75 (2011).
[14] G. Xiong, R. Shao, T. C. Droubay, A. G. Joly, K. M. Beck, S. A. Chambers, and W. P. Hess, Adv. Funct. Mater. **17**, 2133–2138 (2007).
[15] P. Deák, B. Aradi, and T. Frauenheim, J. Phys. Chem. C **115**(8), 3443–3446 (2011).
[16] D. O. Scanlon, C. W. Dunnill, J. Buckeridge, S. A. Shevlin, A. J. Logsdail, S. M. Woodley, C. R. A. Catlow, M. J. Powell, R. G. Palgrave, I. P. Parkin, G. W. Watson, T. W. Keal, P. Sherwood, A. Walsh, and A. A. Sokol, Nature Mater. **12**(9), 798–801 (2013).
[17] V. Pfeifer, P. Erhart, S. Li, K. Rachut, J. Morasch, J. Brötz, P. Reckers, T. Mayer, S. Rühle, A. Zaban, I. Mora Seró, J. Bisquert, W. Jaegermann, and A. Klein, J. Phys. Chem. Lett. **4**(23), 4182–4187 (2013).
[18] T. Frauenheim, G. Seifert, M. Elsterner, Z. Hajnal, G. Jungnickel, D. Porezag, S. Suhai, and R. Scholz, Phys. Status Solidi B **217**(1), 41–62 (2000).
[19] B. Aradi, B. Hourahine, and T. Frauenheim, J. Phys. Chem. A **111**(26), 5678–5684 (2007).
[20] http://www.dftb.org/parameters/download/tiorg/tiorg_0_1.
[21] G. Dolgonos, B. Aradi, N. H. Moreira, and T. Frauenheim, J. Chem. Theory Comput. **6**(1), 266–278 (2010).
[22] J. P. Perdew, K. Burke, and M. Ernzerhof, Phys. Rev. Lett. **77**, 3865 (1996).
[23] A. V. Krukau, O. A. Vydrov, A., F. Izmaylov, and G. E. Scuseria, J. Chem. Phys. **125**, 224106 (2006).
[24] G. Kresse and J. Hafner, Phys. Rev. B **49**, 14251 (1994).
[25] G. Kresse and J. Furthmüller, Comput. Mater. Sci. **6**, 15 (1996).
[26] P. E. Blöchl, Phys. Rev. B **50**, 17953 (1994).
[27] N. A. Deskins, S. Kerisit, K. M. Rosso, and M. Dupuis, J. Phys. Chem. C **111**(26), 9290–9298 (2007).
[28] L. Chen, M. E. Graham, G. Li, and K. A. Gray, Thin Solid Films **515**(3), 1176–1181 (2006).
[29] G. Li, N. M. Dimitrijevic, A. Chen, J. M. Nichols, T. Rajh, and K. A. Gray, J. Amer. Chem. Soc. **130**, 5402–5403 (2008).
[30] A. Franciosi and Ch. G. Van de Walle, Surf. Sci. Rep. **25**, 1–140 (1966).
[31] P. Deák, B. Aradi, and T. Frauenheim, Phys. Rev. B **83**(15), 155207 (2011).
[32] P. Deák, B. Aradi, and T. Frauenheim, Phys. Rev. B **86**(19), 195206 (2012).

